JVI Journals.ASM.org

Mutational Mapping of pUL131A of Human Cytomegalovirus Emphasizes Its Central Role for Endothelial Cell Tropism

Andrea Schuessler,[a]* Kerstin Laib Sampaio,[a] Sarah Straschewski,[b] and Christian Sinzger[b]

Institute of Medical Virology and Epidemiology of Virus Diseases, University of Tuebingen, Tuebingen, Germany,[a] and Institut für Virologie, Universität Ulm, Ulm, Germany[b]

The UL131A protein is part of a pentameric variant of the gcIII complex in the virion envelope of human cytomegalovirus (HCMV), which has been found essential for efficient entry into endothelial cells (ECs). Using a systematic mutational scanning approach, we aimed to define peptide motifs within the UL131A protein that contribute to EC infection. Mutant viruses were generated in which charged amino acids within frames of 2 to 6 amino acids were replaced with alanines. The resulting viruses were evaluated with regard to their potential to infect EC cultures. Four clusters of charged amino acids essential for EC infection were identified (amino acids 22 to 27, 32 to 35, 64 to 69, and 116 to 121). Mutations of individual charge clusters within amino acids 72 to 104 caused minor reductions of EC tropism, but these effects were additive in a combined mutation, showing that this region also contributes to EC tropism. Only charge clusters within amino acids 46 to 58 were found irrelevant for EC infection. In conclusion, the unusual sensitivity to mutations, together with the remarkable conservation of the UL131A protein, emphasizes its particular role for EC tropism of HCMV.

Human cytomegalovirus (HCMV) is a member of the betaherpesvirus subfamily and hence causes lifelong persistent infections with episodes of reactivation that are usually well controlled by the immune system. However, under conditions of compromised immunity, HCMV can disseminate hematogenously and infect virtually any organ due to its very broad cell tropism. This broad *in vivo* cell tropism is reflected by clinical isolates of HCMV, which can typically also infect a variety of human cultured cell types, including endothelial cells (ECs) (17, 25–27). Extensive propagation in fibroblast cell cultures regularly entails loss of the EC tropism (31, 36), and this phenotypic alteration is due to mutations within the viral UL128 locus (7, 10). This highly conserved gene region is composed of three open reading frames (ORFs): UL128, UL130, and UL131A (2, 10, 18, 32, 37). The respective proteins, pUL128, pUL130, and pUL131A, form a viral envelope complex with glycoproteins gH and gL, which were first described to complex with glycoprotein gO and were recently also found without any complex partner (1, 12, 13, 19, 38, 40). Virions of poorly endotheliotropic fibroblast-adapted HCMV strains bear only gH/gL/gO and/or gH/gL complexes in their envelope, whereas highly endotheliotropic strains additionally produce virions containing the pentameric gcIII variant gH/gL/pUL128-131 (24). Each of the three genes within the UL128-131 locus is essential for EC tropism, most likely because only a complete pentameric gcIII complex can efficiently mediate endocytic entry in ECs (10, 19). We have previously defined tropism-relevant peptides within UL128 and UL130 by charge-cluster-to-alanine (CCTA) mutagenesis (22, 23), and we report here the completion of this analysis with functional mapping of UL131A.

UL131A is disrupted in AD169 (8), causing a loss of endothelial cell tropism in this widely used laboratory strain (10). Repair of UL131A reconstitutes the capability to infect cultured endothelial and epithelial cells, at the cost, however, of a delayed and/or reduced release of virus progeny from infected cultures (1, 37). Loss of a functional UL131A gene obviously represents a selective advantage in fibroblasts. In line with this interpretation, the occurrence of mutations in UL131A during extended propagation in fibroblasts was recently confirmed with two other HCMV isolates (7). The role of the UL131A-encoded protein (pUL131A) within the pentameric envelope complex gcIII has been studied by a coprecipitation analysis (19). Apparently, all three proteins of the UL128 locus are assembled onto a core complex of gH and gL (1, 38), and it is particularly pUL131A that requires the previous complexing of gH/gL for binding (19). The pUL131A protein also bound to pUL130 in the latter study, and this interaction appeared to be a covalent binding via disulfide bonds (19). Without pUL131A, gH/gL/pUL128/pUL130 complexes were formed in the cell but were not further matured (19). It appeared that pUL131A has a particularly central role within the pentameric tropism-relevant gcIII, hence making it an attractive objective for antiviral strategies targeting inhibition of EC infection. A prerequisite for such interventions is the identification of peptides within pUL131A that contribute to EC tropism. To this end, we generated an array of virus mutants carrying charge-cluster-to-alanine replacements within UL131A and characterized them with regard to their ability to infect ECs. The results emphasize the particular role of pUL131A with the remarkable finding that 7 of 9 mutations caused a reduction of EC tropism.

MATERIALS AND METHODS

Cells and viruses. Human foreskin fibroblasts (HFFs) were cultured in minimal essential medium (MEM) (GIBCO/Invitrogen) containing 5% fetal calf serum (FCS), 2.4 mmol/liter glutamine, 100 μg/ml gentamicin, and 0.5 ng/ml basic fibroblast growth factor (bFGF) (GIBCO/Invitrogen).

Received 9 June 2011 Accepted 14 October 2011

Published ahead of print 26 October 2011

Address correspondence to Christian Sinzger, christian.sinzger@uniklinik-ulm.de.

* Present address: Australian Infectious Diseases Research Centre, School of Chemistry and Molecular Biosciences, University of Queensland, Brisbane, Australia.

doi:10.1128/JVI.05354-11

TABLE 1 Primers used for markerless mutagenesis of TB40-BAC4-UL131A

Mutant BAC	Primer direction	Primer sequence[a]
TB40-BAC4-UL131ccta22-27	Forward	GTCTGTTTGTCTGTGCGCCGTGGTGCTGGGTCAGTGCCAG**GCAGCAACCGCAGCAAG**CAAACGATTATTACCGAGTtACCaggatgacgacgataagt
	Reverse	AGCACGGCTCCCAGTAATGCGGTACTCGGTAATAATCGTTT**GCTGCTGCGGTTGCTGC**CTGGCACTGACCCAGCACCAcaaccaattaaccaattctga
TB40-BAC4-UL131ccta32-35	Forward	TCAGTGCCAGCGAGAGACCGCAGAAAAAAACGATTATTACG**GCAGTACCGGCA**TACTGGGACGCGTGCTCTCGaggatgacgacgataagt
	Reverse	GGGTTTGGTCGGGCAGCGCGCGAGACGGCTCCCAGTAT**GCCGGTACTGCC**GTAATAATCGTTTTTTTCTGcaaccaattaaccaattctga
TB40-BAC4-UL131ccta46-51	Forward	AGTACCGCATTACTGGGACGCATGCTCTCGCGCGCTGCCC**GCACAAACCGCATACGCA**TATGTGGAACAGCTCGTGAaggatgacgacgataagt
	Reverse	AGTGGTAGTTCAACGTGAGGTCCACGAGCTGTTCCACATAT**GCGTATGCGGTTTGTGC**GGGCAGCGCGCGAGACATGcaaccaattaaccaattctga
TB40-BAC4-UL131ccta54-58	Forward	CTCTCGCGCGCTGCCCGACCAAACCCGTTACAAGTATGTG**GCACAGCTCGTGGCA**CTCACGTTGAACTACCACTAaggatgacgacgataagt
	Reverse	CCAAGCCGTGGCTCGCATCGTAGTGGTAGTTCAACGTGAG**TGCCACGAGCTGTGC**CACATACTTGTAACGGGTTTcaaccaattaaccaattctga
TB40-BAC4-UL131ccta64-69	Forward	CAAGTATGTGGAACAGCTCGTGGACCTCACGTTGAACTAC**GCATACGCAGCGAGCGCA**GGCTTGGACAACTTTGACGTaggatgacgacgataagt
	Reverse	CGTATCCTCACCTCTTGAGCACGTCAAAGTTGTCCAAGCC**TGCGCTCGCTGCGTATGC**GTAGTTCAACGTGAGGTCCAcaaccaattaaccaattctga
TB40-BAC4-UL131ccta72-75	Forward	CCTCACGTTGAACTACCACTACGATGCGAGCCACGGCTTG**GCAAACTTTGCA**GTGCTCAAGAGGTGAGGATAaggatgacgacgataagt
	Reverse	TGTCATACACCTTTAGCGCGTATCCTCACCTCTTGAGCAC**TGCAAAGTTTGC**CAAGCCGTGGCTCGCATCGTcaccaattaccaattctga
TB40-BAC4-UL131ccta93-98	Forward	AATCAACGTGACCGAGGTGTCGTTGCTCATCAGCGACTTT**GCAGCACAGAAACGCAGCA**GGCGGCACCAACAAAAGGACaggatgacgacgataagt
	Reverse	AACCTGCGGCGCGTTGAACGTGGTCCTTTTGTTGGTGCCGCCT**GCTGCGTTCTGTGCTGC**AAAGTCGCTGATGAGCAACGcaaccaattaaccaattctga
TB40-BAC4-UL131ccta103-104	Forward	CAGCGACTTTAGACGTCAGAACCGTCGCGGAGGCACCAAC**GCAGC**AACCACGTTCAACGCGCGCCGCGaggatgacgacgataagt
	Reverse	GGGCGTGCGGTGCCAGCGAACCGGCGGCGTTGAACGTGGTTG**CTGC**GTTGGTGTCCTCCGCGACGGTcaaccaattaaccaattctga
TB40-BAC4-UL131ccta116-121	Forward	CAAAAGGACCACGTTCAACGCAGCAGGTTCGCTGGCGCCG**GCAGCAAGCCTAGCA**TTCAGCGTGCGGCTCTTTGCaggatgacgacgataagt
	Reverse	CCCGTGACGCAGGCTAGTTGGCAAAGAGCCGCACGCTGAA**TGCTAGGCTTGCTGCTGC**GGCGCCAGCGAACCTGCTGcaaccaattaaccaattctga

[a] Note: uppercase letters, HCMV homology; lowercase letters, homology to template plasmid pEP-Kan-S; bold letters, sequence of interest.

Human umbilical vein endothelial cells (HUVECs) were cultured in RPMI 1640 (GIBCO/Invitrogen) with 50 μg/ml endothelial cell growth supplement (ECGS) (Becton Dickinson), 10% human serum (HCMV seronegative), 5 IU/ml heparin, and 100 μg/ml gentamicin. HCMV strain TB40-BAC4 and derived mutants were propagated in HFFs. Virus stocks were prepared by harvesting infectious supernatants from HFF cultures at days 5 to 7 postinfection. Cell debris was removed by centrifugation (3,220 $\times$ *g*, 10 min), and the clarified supernatants were then stored at −80°C until used for phenotypic characterization.

Markerless mutagenesis of HCMV genomes. For generation of mutant virus strains, we used the HCMV-TB40/E-derived bacterial artificial chromosome (BAC) TB40-BAC4, which is highly EC-tropic (28). Mutant BACs were generated by applying the markerless mutagenesis protocol of Tischer et al. (35). Briefly, recombination fragments were generated by PCR from plasmid pEP-Kan-S. Primers were designed to replace codons for charged amino acids in the sequence of interest by codons for alanine (Table 1). The resulting fragments consisted of the 18-bp I-Sce I restriction site and a kanamycin resistance cassette flanked by overlapping HCMV homologies each containing the sequence of interest. The recombination fragments were inserted into TB40-BAC4 by homologous recombination in *Escherichia coli* strain GS1783 (34). Following kanamycin selection, all non-HCMV sequences were removed by an intrabacterial I-Sce I digest and a subsequent red recombination. Correctness of each mutation was confirmed by sequencing of the complete UL131A reading frame. For reconstitution of infectious virus, BAC-DNA was isolated using the NucleoBond Xtra Midi kit (Macherey-Nagel) and transfected into HFFs using the MBS transfection kit (Stratagene). Transfected cells were propagated and virus was harvested when the viral cytopathic effect had grown to almost 100%. To control for unwanted mutations in the UL128-131A region during reconstitution or passaging in HFFs, we have analyzed the complete sequence of the UL128-131A region in each of the mutant viruses using Hirt lysates of infected HFFs as a template (11). No alterations were found in UL128 or UL130 with any of the mutants. In UL131A, only the desired mutations were found in each of the mutant viruses.

Measurement of endothelial cell tropism. For evaluation of cell-free infectivity of the respective mutants in HUVECs and HFFs, cells were seeded 1 day prior to the experiment at 2×10^4/well in 96-well plates coated with 0.1% gelatin. Cells were preincubated for 30 min at 37°C with MEM and then infected with the respective virus suspension for 2 h. The virus suspension was replaced with fresh medium, and infected cultures were incubated overnight at 37°C. For detection of viral immediate-early antigen (pUL122/123), cells were fixed with 80% acetone and incubated sequentially with antibody E13 (Biosoft) and Cy3-conjugated goat anti-mouse IgG $F(ab')_2$ (Jackson ImmunoResearch). Nuclei were counterstained with 4′,6-diamidino-2-phenylindole (DAPI). The infection efficiency in HFFs and HUVECs was quantified, and the relative EC tropism of the mutant viruses in comparison to that of the wild-type HCMV-TB40-BAC4 was determined by calculating the ratio of infection efficiencies in HUVECs and HFFs.

Cell-associated viral spread in EC monolayers was tested by a focus expansion assay essentially as described previously (30). Infected fibroblasts were cocultured with uninfected ECs for 5 days in gelatin-coated 96-well plates and then fixed and stained for immediate-early antigen and DAPI as described above. The average number of infected cells per focus (FE_{HUVEC}) was quantified.

Purification of HCMV virions by glycerol-tartrate gradient. Virion fractions were isolated from late-stage-infected cell culture supernatants by glycerol-tartrate density gradients essentially as described previously (33). Briefly, 60 to 120 ml of infectious supernatants was centrifuged at 3,220 $\times$ *g* for 10 min to remove cellular debris. HCMV particles were then pelleted by ultracentrifugation at 80,000 $\times$ *g* for 70 min. The pellets were resuspended in 2 ml sodium phosphate buffer (8 mM $NaH_2PO_4 \cdot 1H_2O$, 32 mM $Na_2HPO_4 \cdot 12H_2O$, pH 7.4) and layered onto a preformed linear glycerol-tartrate gradient (15% sodium tartrate/30% glycerol to 35% sodium tartrate in phosphate buffer). The gradient was centrifuged at

FIG 1 Charge clusters in the amino acid sequence of pUL131A of TB40-BAC4. Charged amino acids are indicated by bold letters. Six charge clusters were identified in pUL131A and are highlighted in gray. Boxed amino acids represent the motifs chosen for CCTA mutagenesis (i.e., amino acids 22 to 27, 32 to 35, 46 to 51, 54 to 58, 64 to 69, 72 to 75, 93 to 98, 103 to 104, 116 to 121). Colors indicate the phenotypes of the CCTA mutants: green, no phenotype; yellow, intermediate phenotype; red, severe phenotype. The underlined sequence marks the predicted signal peptide.

80,000 × *g* for 45 min, resulting in separation of HCMV particles into noninfectious enveloped particles (NIEPs), virions, and dense bodies. The virion fraction was collected using a syringe and needle, resuspended in phosphate buffer, and recentrifuged at 80,000 × *g* for 70 min. The supernatant was discarded, and the virion pellets were stored at −80°C until being used for Western blot analyses.

Western blot analyses. For detection of viral proteins in infected fibroblasts, cells were lysed for 30 min on ice with RIPA buffer (50 mM Tris, pH 7.4, 150 mM NaCl, 1 mM EDTA, 01% SDS, 0.5% deoxycholate, 1% NP-40) containing protease inhibitors. For detection of viral proteins in virus particles, gradient-purified virions were lysed for 30 min on ice with RIPA buffer containing protease inhibitors. Protein concentrations were determined with a precision red advanced protein assay (Cytoskeleton). Equal amounts of cell or viral extracts were separated in 12% SDS-polyacrylamide gels and blotted onto polyvinylidene difluoride (PVDF) membranes (Bio-Rad Laboratories). Membranes were blocked with phosphate-buffered saline (PBS) containing 0.3% Tween 20 and 5% dry milk powder and incubated with the indicated monoclonal or polyclonal antibodies followed by peroxidase-conjugated goat anti-mouse (Pierce Biotechnology) or goat anti-rabbit (Millipore Corp) IgGs. A monoclonal antibody (MAb) specific for pUL128 (MAb 17) was a gift from Giuseppe Gerna (Fondazione IRCCS Policlinico San Matteo, Pavia, Italy). The mouse MAb directed against pUL130 was a gift from Dai Wang and Tom Shenk (Department of Molecular Biology, Princeton University, Princeton, NJ). Rabbit polyclonal antiserum directed against pUL131A was a gift from Brent Ryckman (Oregon Health and Science University, Portland, OR). As an internal loading control, an MAb directed against gB (GeneTex) was used. A chemiluminescence detection kit (SuperSignal West Dura; Pierce Biotechnology) was used according to the manufacturer's instructions, and signals were visualized by exposition of Kodak X-Omat X-ray films.

Immunofluorescence detection of virus particles in infected cells. We utilized detection of the capsid-associated tegument protein pUL32 (3) for visualization of virus particles during the entry phase as previously described (21, 29) and applied by other groups (14, 15). Assays were performed at a multiplicity of infection of 5 to 15. In order to limit the fraction of biologically inactive particles in the virus preparations, producer cultures were washed and incubated with fresh medium overnight. Infectious supernatants were then harvested, clarified of cell detritus, and used for experiments. Target cells were seeded on gelatin-coated 96-well μclear plates (Greiner Bio-One) one day prior to the experiment. The following day, medium was removed and cell-free virus preparations were added. After 1 h, nonbound virus was removed and cells were washed with MEM and either fixed or incubated for an additional 5 h in fresh medium. Fixation was done by incubation with 80% acetone for 5 min at ambient temperature followed by three washes with PBS. For immunofluorescence detection of viral particles, fixed cell cultures were first incubated with MAb XP1 directed against the capsid-associated HCMV-tegument protein pp150 (pUL32; Behringwerke), washed with PBS, and then incubated with Alexa Fluor 488-conjugated goat anti-mouse IgG $F(ab')_2$ (Molecular Probes). Nuclei were counterstained with DAPI, and stainings were visualized under a Zeiss Axiovert 200 microscope and documented using Axiovision software. In three individual experiments, virions from a minimum of 25 cells per condition were counted according to their subcellular localization.

Statistical analysis. To test for statistical significance of differences in cell tropism values of the various viruses, two-tailed Mann-Whitney *U* test analyses were performed. A *P* value of <0.05 was considered marginally significant, a *P* value of <0.01 was considered significant, and a *P* value of <0.001 was considered highly significant.

RESULTS

Identification of charge clusters in pUL131A and generation of mutants. Charge-cluster-to-alanine (CCTA) scanning is a systematic mutational approach focusing on sites that are likely exposed on the surface of a protein (4). While gross deletions or mutations in uncharged parts of the protein tend to destroy the overall structure of a protein and are hence noninformative with regard to functional mapping, replacement of charged amino acids with uncharged alanines is assumed to preserve the backbone of the protein and alter specifically potential interaction sites on the protein surface (6). Following definition of a charge cluster as at least two charged amino acids within five successive amino acids (39), we could identify six charge clusters in TB40-BAC4 pUL131A (Fig. 1). From each charge cluster, a sequence of up to six amino acids was chosen for CCTA mutagenesis, except the first charge cluster, as this is part of a predicted signal peptide that is cleaved off. Several sites were chosen from charge clusters 2 and 3, because they are particularly large (indicated by boxes in Fig. 1). Designation of motifs chosen for CCTA scanning indicates their amino acid positions: $RETAEK_{22-27}$, $RVPH_{32-35}$, $DQTRYK_{46-51}$, $EQLVD_{54-58}$, $HYDASH_{64-69}$, $DNFD_{72-75}$, $RRQNRR_{93-98}$, $KR_{103-104}$, and $HARSLE_{116-121}$. Mutant viral genomes were generated in *E. coli* containing the BAC HCMV-TB40-BAC4 (28) by seamlessly replacing the selected charged amino acids with alanines (Table 2). All mutants carried the desired mutations as tested by sequencing of UL131A from BAC-DNAs. Mutant BAC genomes were then transfected into human foreskin fibroblasts (HFFs) for reconstitution of virus. The transfected HFFs showed viral plaques within 5 to 10 days after transfection and grew to 100% cytopathic effect (CPE) during further cell culture passages. As UL131A is dispensable for replication of HCMV in fibroblasts, transfection of mutant viruses always yielded high-titer virus preparations of $>10^6$ infectious units per ml. Stocks of each virus were produced in HFFs and stored at −80°C for phenotypic testing in HFFs and ECs. The integrity of the UL128-131A gene region

TABLE 2 Overview of TB40-BAC4-UL131ccta mutants and their respective amino acid exchanges

Amino acids[a]	CCTA mutation	Mutant TB40-BAC4
RETA**EK**	AATAAA	-UL131ccta22-27
RVPH	AVPA	-UL131ccta32-35
DQTRYK	AQTAYA	-UL131ccta46-51
EQLV**D**	AQLVA	-UL131ccta54-58
HYDASH	AYAASA	-UL131ccta64-69
DNF**D**	ANFA	-UL131ccta72-75
RRQN**RR**	AAQNAA	-UL131ccta93-98
KR	AA	-UL131ccta103-104
HARSL**E**	AAASLA	-UL131ccta116-121

[a] Amino acids changed in the CCTA mutants are in bold.

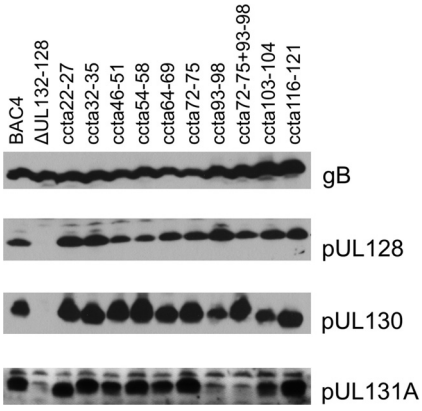

FIG 2 Expression of UL128-131A proteins in cells infected with CCTA mutant viruses. Lysates of HFFs infected with the various UL131ccta mutants were analyzed by immunoblotting for the presence of pUL128, pUL130, pUL131A. Anti-gB served as a control antibody. Wild-type HCMV-TB40-BAC4 and a mutant lacking the complete UL128-131A gene region (22) served as positive- and negative-control viruses, respectively.

was verified by determining the DNA sequence of ORFs UL128, UL130, and UL131A in Hirt lysates from HFF infected with the respective virus stocks. No unwanted mutations were detected in either of the ORFs with any of the mutants. All reconstituted mutants, however, still carried the desired UL131A mutation that we had introduced into the BACs. Infected cells were tested for expression of the mutated genes by immunoblotting of protein lysates using antibodies against pUL128, pUL130, and pUL131A. All mutants expressed pUL128 and pUL130 to an extent indistinguishable from wild-type virus. Also, the mutated UL131A proteins were detectable at wild-type levels with all mutants except those carrying the ccta93-98 mutation, which did not give a signal above background level of the UL132-128 deletion mutant (Fig. 2). This may indicate either a lack of expression or disruption of the epitope against which the antibody is reactive (see Discussion).

Endothelial cell tropism of HCMV-TB40-BAC4-UL131ccta mutants. We evaluated the effect of each mutation on replication of the respective virus in ECs by repeated testing of cell-free virus preparations on HUVECs and HFFs in parallel. As UL131A is known to be dispensable for infection of fibroblasts (10), we chose fibroblast infection as a reference reflecting the amount of infectious virus within a given virus preparation. The ratio of infection rates in both cell types was then taken as an indicator of the "relative EC tropism" of each mutant.

The effects of charge cluster mutations introduced into UL131A can be sorted into three categories: those without alteration of EC tropism (Fig. 1, green boxes), those causing a moderate reduction of EC tropism (Fig. 1, yellow boxes), and those severely reducing EC tropism of the respective mutant (Fig. 1, red boxes). An example of each category of mutation is given in Fig. 3A. With regard to the distribution of the various categories of mutations over the length of the UL131A protein, three domains can be discriminated: charged amino acids within the first domain reaching from amino acid (aa) 22 to aa 35 appear to be absolutely essential for EC tropism. In contrast, charged amino acids within the second domain (aa 46 to 58) are dispensable for this phenotype. The third domain, consisting of the C-terminal half of the protein, was sensitive to any changes. CCTA mutations within the central part of this domain (i.e., aa 72 to 75, 93 to 98, or 103 to 104) had a moderate effect, whereas CCTA mutations in the flanking regions were absolutely deleterious to EC tropism of the respective mutants (Fig. 3B).

For two mutants representing the complete loss of EC tropism (HCMV-BAC4-UL131ccta64-69) or the partial reduction of EC tropism (HCMV-BAC4-UL131ccta72-75), we have analyzed the presence of the three UL128-131A proteins in virion particles (Fig. 3C). In gradient-purified virions of the ccta64-69 mutant, none of the proteins could be detected, whereas the gB signal was indistinguishable from signals of wild-type virions. In contrast, virions of the ccta 72-75 mutant contained all three proteins, although at a slightly reduced level.

Revertant viruses were constructed to exclude the possibility that the change in EC tropism of the CCTA mutants was due to unspecific second-site mutations. Again, markerless mutagenesis was applied to restore the wild-type sequence. The relative EC tropism of all revertant viruses was indistinguishable from that of the wild-type HCMV-TB40-BAC4, thus proving that the phenotypic changes of the mutants were caused by the respective charge cluster mutations. One revertant is included in Fig. 3B, being representative of all others.

In summary, the amino acid sequence of UL131A appeared remarkably sensitive to even minor changes with regard to the endotheliotropic phenotype, which is consistent with the almost perfect conservation of its amino acid sequence among clinical HCMV isolates (complete identity on the amino acid level in 11 of 12 randomly selected sequences from four different countries; data not shown).

Additive effect of mutations in $DNFD_{72-75}$ and $RRQNRR_{93-98}$. The CCTA scanning of UL131A had yielded three charge clusters in the region from D72 to R104, mutation of which moderately reduced EC tropism. We assumed that a combination of two mutations from this site would result in a stronger reduction of EC tropism. The aim of such a combination was the generation of a mutant with an intermediate degree of EC tropism in the range between the full-blown reduction to a relative EC tropism of 0.03 and an only moderate reduction to 0.4.

Starting from BAC4-UL131ccta72-75, $RRQNRR_{93-98}$ was mutated to $AAQNAA_{93-98}$ exactly as done previously for generation of the single mutant BAC4-UL131ccta93-98. The resulting dual mutant, BAC4-UL131ccta72-75ccta93-98, could be reconstituted and infectious supernatant could be harvested, which was then tested for its relative EC tropism. As expected, the combination of both mutations had a stronger effect on the EC tropism than the respective single mutations (Fig. 4A). The relative EC tropism of HCMV-BAC4-UL131ccta72-75ccta93-98 was reduced from 0.8 (wild-type HCMV-TB40-BAC4) to 0.13 compared to 0.45 of BAC4-UL131ccta72-75 and 0.36 with BAC4-UL131-UL131ccta93-98. The differences between the dual mutant and each of the single mutants were significant at P values of 0.003 and 0.008, respectively.

To further corroborate this finding, the phenotype was independently quantified by an alternative method, namely, a focus expansion assay measuring the capacity to form infectious foci in HUVEC monolayers, i.e., allowing for cell-associated transmission over a period of 5 days (Fig. 4B). Single mutations ccta72-75 and ccta93-98 reduced focus size roughly by a factor of 2, from 71 infected cells/focus (wild-type HCMV-TB40-BAC4) to 31 and 40

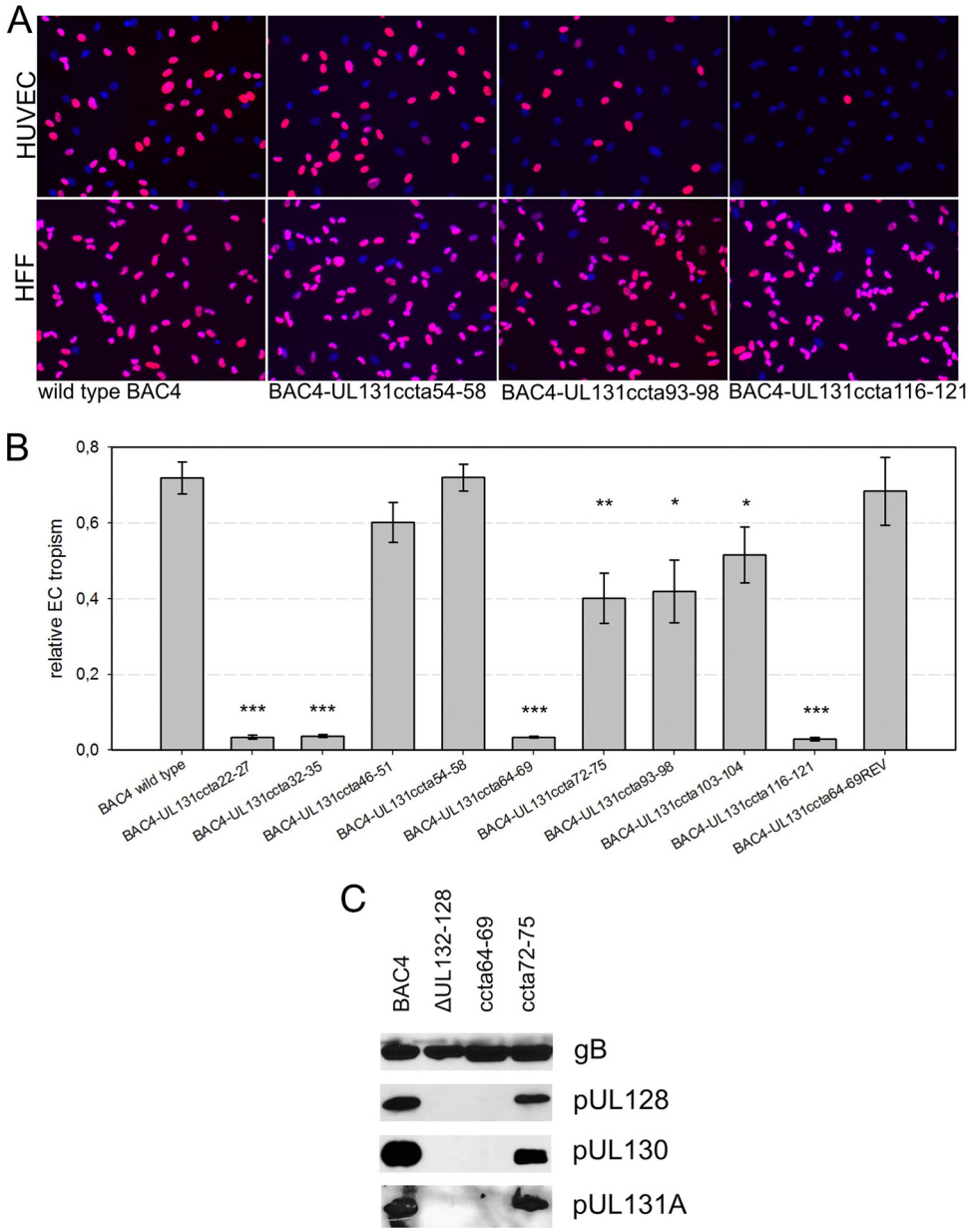

FIG 3 Relative endothelial cell tropism of UL131ccta mutants. Fibroblasts (HFFs) and endothelial cells (HUVECs) were infected by various UL131ccta mutants at a multiplicity of infection of 2.5 infectious units/cell. One day after infection, viral immediate-early antigens were detected by indirect immunofluorescence staining (Cy3, red nuclear signals). Cell nuclei were counterstained with DAPI (blue nuclear signals). (A) Infection efficiency in HUVEC and HFF. One example for each phenotype category is shown: wild-type, HCMV-TB40-BAC4; no phenotype, HCMV-TB40-BAC4-UL131ccta54-58; intermediate phenotype, HCMV-TB40-BAC4-UL131ccta93-98; strong phenotype, HCMV-TB40-BAC4-UL131ccta116-121. (B) Relative EC tropism of all UL131ccta mutants, determined as the ratio of infection efficiency in HUVECs and infection efficiency in HFFs. Bars represent mean values from at least three experiments (standard error of the mean is indicated with each bar). Asterisks indicate a highly significant (***, $P < 0.001$), significant (**, $P < 0.01$) or marginally significant (*, $P < 0.05$) difference between the wild-type virus and the marked mutant. (C) Detection of UL128-131A proteins in virion particles of mutants with complete or partial reduction of EC tropism. Lysates of gradient-purified virions of HCMV-TB40-BAC4-UL131ccta64-69 and HCMV-TB40-BAC4-UL131ccta72-75 were analyzed by immunoblotting for the presence of pUL128, pUL130, and pUL131A. Anti-gB served as a control antibody. Wild-type HCMV-TB40-BAC4 and a mutant lacking the complete UL128-131A gene region (22) served as positive- and negative-control viruses, respectively.

infected cells/focus, respectively. The dual mutation had an additive effect, reducing focus size by a factor of 4, from 71 to 16 cells/focus. The differences between the dual mutant and the single mutants were significant, with P values of 0.019 and 0.004, respectively.

To prove the specificity of the effects, i.e., to exclude second site mutations, two revertants were generated and tested for the relative EC tropism, which almost perfectly resembled the phenotype of wild-type virus (example shown in Fig. 4A).

Analysis of selected mutants with regard to virus binding and entry. In order to address the mechanism by which CCTA mutations in UL131A affect EC tropism, we analyzed two repre-

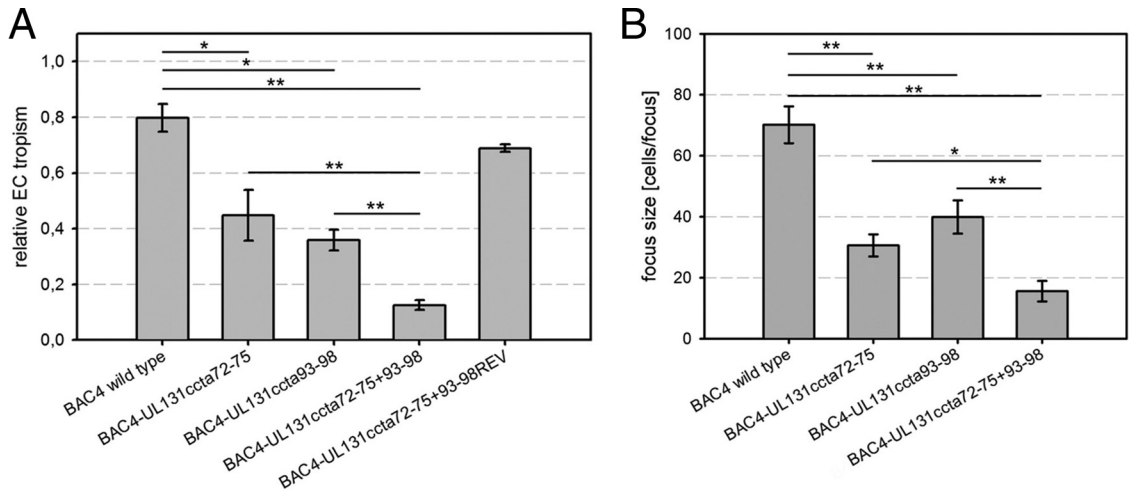

FIG 4 Phenotype of BAC4-UL131ccta72-75ccta93-98 dual mutant. (A) Fibroblasts (HFFs) and endothelial cells (HUVECs) were infected by cell-free preparations of the respective virus at a multiplicity of infection of 2.5 infectious units/cell. One day after infection, viral immediate-early antigens were detected by indirect immunofluorescence staining. The relative EC tropism is given as the ratio of infection efficiency in HUVECs and infection efficiency in HFFs. Bars represent mean values from at least three experiments (standard error of the mean is indicated with each bar). Asterisks indicate a significant (**, $P < 0.01$) or marginally significant (*, $P < 0.05$) difference between the respective viruses. (B) Infected fibroblasts were cocultured with an excess of uninfected ECs (ratio of infected HFFs and uninfected ECs, 1/500) for 5 days and then stained for viral immediate-early antigen. The focus expansion capacity in endothelial cell monolayers is given as the average number of infected cells per focus. Bars represent mean values from at least three experiments (standard error of the mean is indicated with each bar). Asterisks indicate a significant (**, $P < 0.01$) or marginally significant (*, $P < 0.05$) difference between the respective viruses.

sentative mutants with regard to the total number of virus particles binding to HFF and HUVEC and with regard to their ability to translocate toward the nucleus of the respective cell type. As previous experience had shown that nuclear translocation does not exceed random distribution at 1 h of incubation, we chose this time point to analyze the overall binding. We preferred incubation with virus at 37°C to incubation at 4°C, as the latter condition would completely disrupt the microtubule skeleton and might hence cause artifacts. After the 1-h incubation period, unbound virus was removed by washing and cells were either fixed immediately to assess the total number of bound virus or further incubated for 5 h to determine the fate of initially bound viruses. Virus particles were visualized by immunofluorescence detection of the capsid-associated tegument protein pUL32 and analyzed with regard to their subcellular localization. Nuclear translocation was regarded as "successful" entry.

Both mutants could bind to HFFs and ECs with efficiencies similar to that of the marker-rescued positive-control virus (Fig. 5A and C). At the end of the incubation period, the fraction of particles located at the nucleus reflected the number expected from a random distribution over the cell. This pattern had changed greatly after an additional 5 h in HFFs (Fig. 5B and C). Remarkably, the total number of virions was reduced to 40% of the initial load at 6 h postinfection (p.i.). Of the remaining particles, both mutants had efficiently translocated toward the nucleus (70 to 75%), which was similar to the translocation efficiency of the control virus. In contrast, in HUVECs mutants and control virus differed significantly with regard to particle distribution at 6 h p.i. The total number of particles was reduced to 25% of the initial load with the control virus compared to 12% with both mutants. In addition, the fraction of particles located at the nucleus was significantly lower with mutants (7 to 8%) than with control virus (50%). While the former still was indistinguishable from a random distribution over the cell, the latter represented specific translocation toward the nucleus.

DISCUSSION

We report here the functional scanning of pUL131A of HCMV by charge-cluster-to-alanine mutagenesis with regard to EC tropism. Only a small portion of the second charge cluster (aa 46 to 58) seemed to be irrelevant for endothelial cell infection, while mutation of all of the other analyzed charge clusters influenced the ability of the mutant viruses to infect ECs. The effects ranged from intermediate phenotypes (aa 72 to 104) to complete destruction of EC tropism (aa 22 to 35, aa 64 to 69, and aa 116 to 121). The finding that virtually all parts of the UL131A protein are relevant for endothelial cell infection is supported by comparison of the amino acid sequence of pUL131A in clinical isolates of HCMV from different geographical regions that showed that the pUL131A sequence of 11 of 12 clinical isolates is absolutely identical (data not shown). In contrast, comparison of the amino acid sequence of pUL130 in the same clinical isolates showed variation in 12 amino acid positions, mainly in the N-terminal and central part of pUL130, and the function for EC tropism was mapped to the C-terminal third of pUL130, which was again highly conserved (22).

UL131A is part of the gene locus UL128-131 that is needed for entry into ECs, epithelial cells, and dendritic cells and for transfer to leukocytes (9, 10, 37). The proteins encoded by UL128 and UL130 have been shown to form a complex with gH and gL present in the viral envelope (38). Later studies showed that pUL131A is also part of this complex (1, 19). There is further evidence that pUL131A serves a dual role not only for entry into target cells but also for release of viral progeny from infected fibroblasts. Repair of the defective UL131A gene in HCMV strain AD169 restored endothelial cell tropism but impaired virus release from fibroblasts (1). The fact that CCTA scanning identified only a small portion of pUL131A as irrelevant might reflect its central role within the pentameric gH/gL/pUL128-131 complex. As part of this complex, pUL131A is anchored to pUL130 and a surface created by gH and

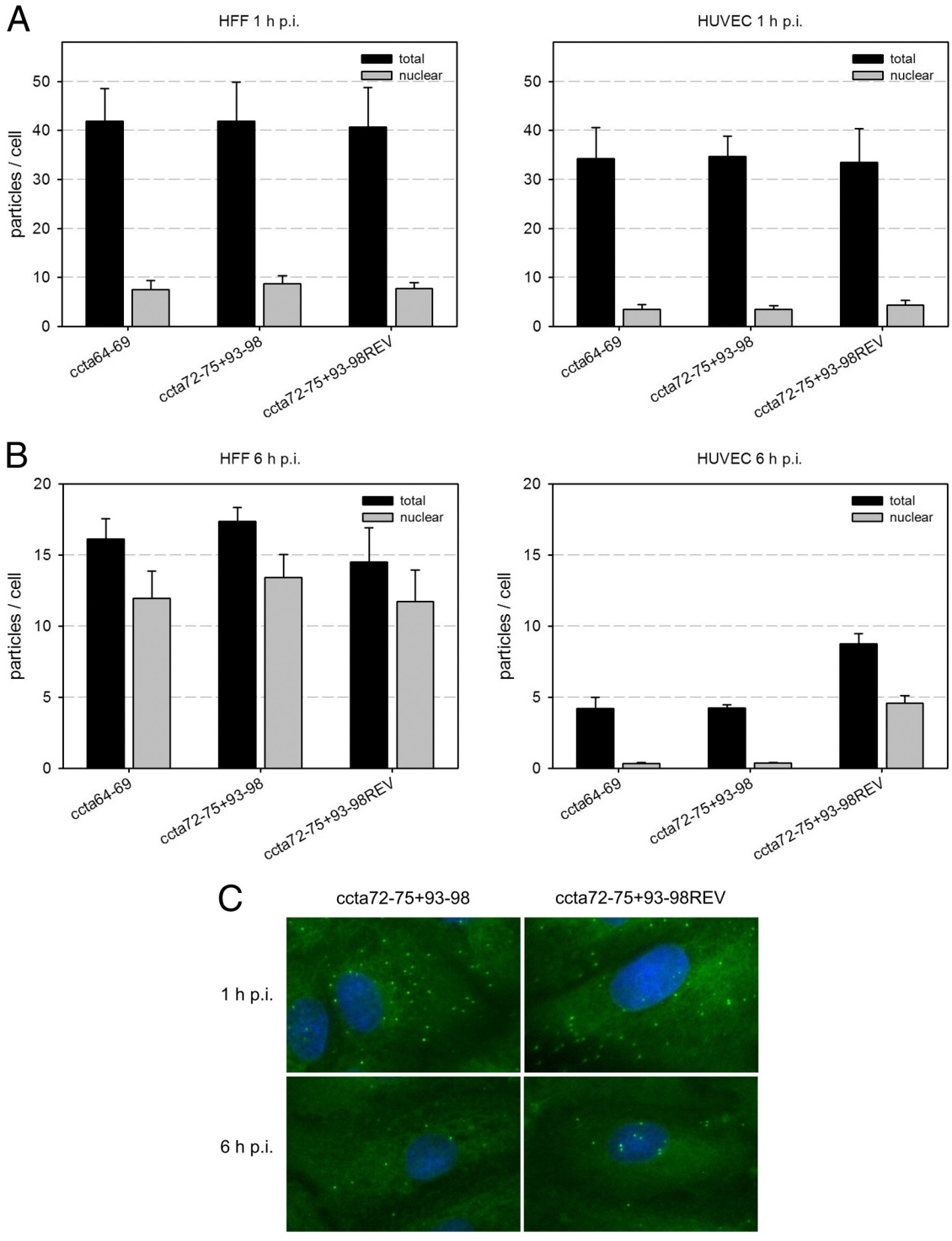

FIG 5 Analysis of virion binding and entry. HFFs and HUVECs were incubated with cell-free supernatants of HCMV-TB40-BAC4-UL131ccta64-69 and HCMV-TB40-BAC4-UL131ccta72-75ccta93-98 for 1 h and then washed and fixed immediately (A) or washed and incubated for further 5 h (B). Virus particles were visualized by immunofluorescence detection of the capsid-associated tegument protein pUL32. The numbers of total particles per cell and particles located at the nucleus were counted. Bars represent mean results of three independent experiments. Standard errors of the means are indicated by error bars. Marker-rescued HCMV-TB40-BAC4-UL131ccta72-75ccta93-98REV served as a positive-control virus. (C) Examples of stainings of HCMV-TB40-BAC4-UL131ccta72-75ccta93-98 and its revertant in HUVECs at 1 h p.i. and 6 h p.i. Bright dot-like green signals represent virus particles; nuclei are counterstained with DAPI.

gL (19). If only one of the UL128-131 proteins is missing, the whole complex is not assembled correctly and consequently missing from virions (19), leading to a loss of EC tropism. It is therefore not unexpected that the non-EC-tropic ccta64-69 mutant lacked all of the three proteins in virion particles despite unaltered expression within infected cells. Obviously, replacement of only three charged amino acids by alanines was sufficient to disrupt correct processing of the pentameric gH/gL complex. CCTA mutants of pUL131A with nonendotheliotropic phenotypes are therefore preferential candidates for the identification of the binding interactions within the complex that is needed for entry into ECs. Future analysis of complex incorporation into virions with the mutations identified here will elucidate their involvement in the interactions with gH/gL and pUL130. The finding that partial loss of EC tropism in the ccta72-75 mutant was associated with reduced incorporation of the three UL128-131A proteins indicates that the degree of EC tropism might be regulated by the amount of gH/gL/pUL128-131A in virions. We have previously reported that poorly EC-tropic HCMV strains can bind to ECs but fail to translocate toward the nucleus (28, 29). Here, we analyzed two EC-tropic CCTA mutants that had lost EC tropism with regard to their entry efficiency, and they showed the same defect found in the previous studies. During a 1-h incubation period, both mutants bound to ECs with the same efficiency as the marker-rescued wild-type control virus. However, after 6 h an accumulation at the nucleus was detectable only with the wild-type virus. In contrast, in HFF, the mutants behaved identically to the wild-type virus. Interestingly, the number of detectable particles after 6 h was greatly reduced compared to the number of initially bound particles and the loss of particles was negatively correlated with the efficiency of nuclear accumulation. This may indicate that attached virions dissociate from the cell if they fail to fuse into the cytoplasm and translocate to the nucleus. Degradation of viral particles is an alternative explanation for the apparent loss of particles during the initial infection phase, and future analyses will have to discriminate between these possibilities.

Concerning those charge clusters not involved in endothelial cell tropism, it is tempting to speculate that they might contribute to the inhibitory function of pUL131A for virus release from fibroblasts. Comparative quantification of virus release from fibroblasts in correlation to the level of endothelial cell tropism of CCTA mutants may help to elucidate the role of specific parts of UL131A in this context. With regard to the generation of attenuated HCMV strains, mutations causing only partial reduction of the EC tropism are of particular interest because previous vaccine trials with low-endotheliotropic HCMV strains have yielded only insufficient immune responses (5, 16). The combination of two of those mutations had an additive effect, thus enabling targeted construction of a virus with the desired degree of EC tropism. Interestingly, a peptide containing charge cluster $pUL131A_{91-98}$ has recently been successfully used to induce neutralizing antibodies in rabbits (20), hence arguing against extended mutation of this epitope for vaccine development. However, as we have previously defined similar mutations with partial effects on the EC tropism in UL128 and UL130 (22, 23), combinations of mutations in different genes are also feasible and may result in an immunogenic mutant that is robust against spontaneous genetic reversion and displays strongly reduced but not completely abrogated replication potential in endothelial cells.

Taken together, the results of this study emphasize the central role of pUL131A for EC tropism of HCMV and provide information on sites within pUL131A that are relevant for this phenotype. This novel information will be useful for further functional characterization of these peptide motifs with regard to interaction of pUL131A with other viral proteins in the gH/gL/pUL128-131 complex and the role of pUL131A for cell-type-specific release of viral progeny. In a clinical context, UL131A mutants with moderately reduced EC tropism are expected to be attenuated but not completely disabled with regard to hematogenous dissemination in the infected host, thus making them promising candidates for the development of a live vaccine strain of HCMV.

ACKNOWLEDGMENTS

We thank Gerhard Jahn for support throughout the study.

This work was supported by the Deutsche Forschungsgemeinschaft through SPP1130, "Infections of the endothelium" (SI 779/3-3).

REFERENCES

1. **Adler B, et al.** 2006. Role of human cytomegalovirus UL131A in cell type-specific virus entry and release. J. Gen. Virol. **87**:2451–2460.
2. **Baldanti F, et al.** 2006. Human cytomegalovirus UL131A, UL130 and UL128 genes are highly conserved among field isolates. Arch. Virol. **151**: 1225–1233.
3. **Baxter MK, Gibson W.** 2001. Cytomegalovirus basic phosphoprotein (pUL32) binds to capsids in vitro through its amino one-third. J. Virol. **75**:6865–6873.
4. **Chothia C.** 1976. The nature of the accessible and buried surfaces in proteins. J. Mol. Biol. **105**:1–12.
5. **Cui X, Meza BP, Adler SP, McVoy MA.** 2008. Cytomegalovirus vaccines fail to induce epithelial entry neutralizing antibodies comparable to natural infection. Vaccine **26**:5760–5766.
6. **Cunningham BC, Wells JA.** 1989. High-resolution epitope mapping of hGH-receptor interactions by alanine-scanning mutagenesis. Science **244**: 1081–1085.
7. **Dargan DJ, et al.** 2010. Sequential mutations associated with adaptation of human cytomegalovirus to growth in cell culture. J. Gen. Virol. **91**: 1535–1546.
8. **Davison AJ, et al.** 2003. The human cytomegalovirus genome revisited: comparison with the chimpanzee cytomegalovirus genome. J. Gen. Virol. **84**:17–28.
9. **Gerna G, et al.** 2005. Dendritic-cell infection by human cytomegalovirus is restricted to strains carrying functional UL131-128 genes and mediates efficient viral antigen presentation to CD8+ T cells. J. Gen. Virol. **86**: 275–284.
10. **Hahn G, et al.** 2004. Human cytomegalovirus UL131-128 genes are indispensable for virus growth in endothelial cells and virus transfer to leukocytes. J. Virol. **78**:10023–10033.
11. **Hirt B.** 1967. Selective extraction of polyoma DNA from infected mouse cell cultures. J. Mol. Biol. **26**:365–369.
12. **Huber MT, Compton T.** 1998. The human cytomegalovirus UL74 gene encodes the third component of the glycoprotein H-glycoprotein L-containing envelope complex. J. Virol. **72**:8191–8197.
13. **Li L, Nelson JA, Britt WJ.** 1997. Glycoprotein H-related complexes of human cytomegalovirus: identification of a third protein in the gCIII complex. J. Virol. **71**:3090–3097.
14. **Miller MS, Hertel L.** 2009. Onset of human cytomegalovirus replication in fibroblasts requires the presence of an intact vimentin cytoskeleton. J. Virol. **83**:7015–7028.
15. **Ogawa-Goto K, et al.** 2003. Microtubule network facilitates nuclear targeting of human cytomegalovirus capsid. J. Virol. **77**:8541–8547.
16. **Plotkin SA.** 1999. Cytomegalovirus vaccine. Am. Heart J. **138**:S484–S487.
17. **Riegler S, et al.** 2000. Monocyte-derived dendritic cells are permissive to the complete replicative cycle of human cytomegalovirus. J. Gen. Virol. **81**:393–399.
18. **Ryckman BJ, Jarvis MA, Drummond DD, Nelson JA, Johnson DC.** 2006. Human cytomegalovirus entry into epithelial and endothelial cells depends on genes UL128 to UL150 and occurs by endocytosis and low-pH fusion. J. Virol. **80**:710–722.
19. **Ryckman BJ, et al.** 2008. Characterization of the human cytomegalovirus

gH/gL/UL128-131 complex that mediates entry into epithelial and endothelial cells. J. Virol. **82**:60–70.
20. **Saccoccio FM, et al.** 2011. Peptides from cytomegalovirus UL130 and UL131 proteins induce high titer antibodies that block viral entry into mucosal epithelial cells. Vaccine **29**:2705–2711.
21. **Sampaio KL, Cavignac Y, Stierhof YD, Sinzger C.** 2005. Human cytomegalovirus labeled with green fluorescent protein for live analysis of intracellular particle movements. J. Virol. **79**:2754–2767.
22. **Schuessler A, Sampaio KL, Scrivano L, Sinzger C.** 2010. Mutational mapping of UL130 of human cytomegalovirus defines peptide motifs within the C-terminal third as essential for endothelial cell infection. J. Virol. **84**:9019–9026.
23. **Schuessler A, Sampaio KL, Sinzger C.** 2008. Charge cluster-to-alanine scanning of UL128 for fine tuning of the endothelial cell tropism of human cytomegalovirus. J. Virol. **82**:11239–11246.
24. **Scrivano L, Sinzger C, Nitschko H, Koszinowski UH, Adler B.** 2011. HCMV spread and cell tropism are determined by distinct virus populations. PLoS Pathog. **7**:e1001256.
25. **Sinzger C, Digel M, Jahn G.** 2008. Cytomegalovirus cell tropism, p 63–83. *In* Shenk TE and Stinski MF (ed), Human cytomegalovirus, vol 325. Springer, Heidelberg, Germany.
26. **Sinzger C, et al.** 2006. Macrophage cultures are susceptible to lytic productive infection by endothelial-cell-propagated human cytomegalovirus strains and present viral IE1 protein to CD4+ T cells despite late down-regulation of MHC class II molecules. J. Gen. Virol. **87**:1853–1862.
27. **Sinzger C, et al.** 1995. Fibroblasts, epithelial cells, endothelial cells and smooth muscle cells are major targets of human cytomegalovirus infection in lung and gastrointestinal tissues. J. Gen. Virol. **76**:741–750.
28. **Sinzger C, et al.** 2008. Cloning and sequencing of a highly productive, endotheliotropic virus strain derived from human cytomegalovirus TB40/E. J. Gen. Virol. **89**:359–368.
29. **Sinzger C, et al.** 2000. Tropism of human cytomegalovirus for endothelial cells is determined by a post-entry step dependent on efficient translocation to the nucleus. J. Gen. Virol. **81**:3021–3035.
30. **Sinzger C, Knapp J, Plachter B, Schmidt K, Jahn G.** 1997. Quantification of replication of clinical cytomegalovirus isolates in cultured endothelial cells and fibroblasts by a focus expansion assay. J. Virol. Methods **63**: 103–112.
31. **Sinzger C, et al.** 1999. Modification of human cytomegalovirus tropism through propagation in vitro is associated with changes in the viral genome. J. Gen. Virol. **80**:2867–2877.
32. **Sun ZR, et al.** 2009. Structure characterization of human cytomegalovirus UL131A, UL130 and UL128 genes in clinical strains in China. Genet. Mol. Res. **8**:1191–1201.
33. **Talbot P, Almeida JD.** 1977. Human cytomegalovirus: purification of enveloped virions and dense bodies. J. Gen. Virol. **36**:345–349.
34. **Tischer BK, Smith GA, Osterrieder N.** 2010. En passant mutagenesis: a two step markerless red recombination system. Methods Mol. Biol. **634**: 421–430.
35. **Tischer BK, von Einem J, Kaufer B, Osterrieder N.** 2006. Two-step red-mediated recombination for versatile high-efficiency markerless DNA manipulation in Escherichia coli. Biotechniques **40**:191–197.
36. **Waldman WJ, et al.** 1991. Preservation of natural endothelial cytopathogenicity of cytomegalovirus by propagation in endothelial cells. Arch. Virol. **117**:143–164.
37. **Wang D, Shenk T.** 2005. Human cytomegalovirus UL131 open reading frame is required for epithelial cell tropism. J. Virol. **79**: 10330–10338.
38. **Wang D, Shenk T.** 2005. Human cytomegalovirus virion protein complex required for epithelial and endothelial cell tropism. Proc. Natl. Acad. Sci. U. S. A. **102**:18153–18158.
39. **Wertman KF, Drubin DG, Botstein D.** 1992. Systematic mutational analysis of the yeast ACT1 gene. Genetics **132**:337–350.
40. **Wille PT, Knoche AJ, Nelson JA, Jarvis MA, Johnson DC.** 2010. A human cytomegalovirus gO-null mutant fails to incorporate gH/gL into the virion envelope and is unable to enter fibroblasts and epithelial and endothelial cells. J. Virol. **84**:2585–2596.